Optomechanical entanglement: How to prepare, verify and "steer" a macroscopic mechanical quantum state?

Stefan Danilishin,[1] Haixing Miao,[2] Helge Müller-Ebhardt,[3] and Yanbei Chen[2]

[1]*School of Physics, University of Western Australia, WA 6009, Australia*
[2]*California Institute of Technology, MC 350-17, Pasadena, California 91125*
[3]*Max-Planck-Institut für Gravitationsphysik (Albert-Einstein-Institut) and Universität Hannover, Callinstr. 38, 30167 Hannover, Germany*

We consider a generic optomechanical system and investigate quantum entanglement between the outgoing light fields and the mechanical motion of the mirror. In contract to traditional approach, we do not consider quantum correlations between the intracavity optical mode and the mechanical motion of a mirror, rather the correlations between the continuum of optical fields in the outgoing light wave and the mechanical degree of freedom. This entanglement is shown to be robust to thermal decoherence and depend on the ratio of measurement strength (light power) and decoherence rate $\propto T/Q_m$. Furthermore, we describe a feasible way to demonstrate quantum state steering, usinging time-variable homodyne detection scheme that allows to evade back-action. An intimate connection between optomechanical steerability and quantum state tomography [Phys. Rev. A **81**, 012114 (2010)] is demonstrated.

I. INTRODUCTION

Optomechanics becomes our gate to the macroscopic quantum world [1]. Recently, experimentalists have successfully cooled the macroscopic oscillator to its ground state using optomechanical interaction [2, 3] and unveiled the hitherto elusive quantum radiation pressure shot noise [4]. These remarkable successes imply that strong non-local quantum correlations first predicted by Einstein, Podolsky and Rosen [5], will soon be seen for really macroscopic mechanical objects in the spirit of original EPR proposal. In fact, the task of demonstration of robust EPR entanglement in optomechanical systems has been attended by many authors [6–12]. In this paper, we focus however on a particular case of correlations arising between the outgoing light fields and the mechanical motion of the centre of mass of a movable mirror in the optical Fabry-Pérot cavity that is not a bipartite entanglement. As the outgoing light comprises a continuum of optical modes, carrying each a tiny bit of information about the mirror's motion, the mechanical degree of freedom finds itself entangled with a continuum of optical degrees of freedom. Following [13], we introduce a mathematical framework for treating quantum entanglement that involves infinite degrees of freedom, and show that this entanglement is suprisingly robust to environmental disturbances and persists for more than one mechanical oscillation period after the optomechanical interaction is turned off, provided that the characteristic frequency of the optomechanical interaction is higher than that of the thermal noise.

We also suggest a way to utilise this entanglement do demonstrate "steering" of a mechanical state — the ability of modifying the quantum state of one party by making different measurements on the other. This is the essence of the Gedankenexperiment of Einstein, Podolsky, and Rosen (EPR) [5], and has been rigorously formulated by Wiseman *et al.* [14–16] as quantum steerability. More recently, Wiseman has shown that steerability can be demonstrated by showing detector-dependent stochastic evolution of a two-level atom coupled to an optical field which in turn is measured continuously [17].
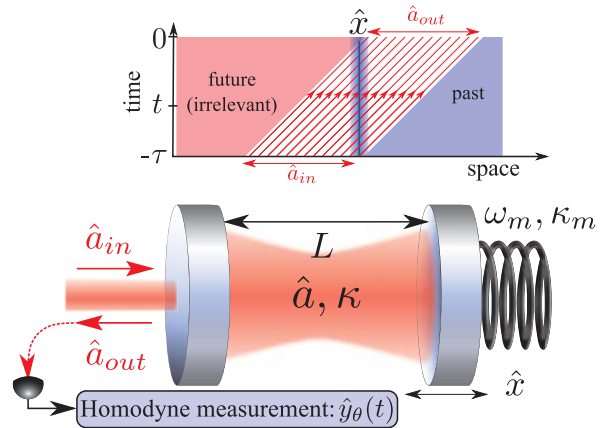

FIG. 1. A typical optomechanical system and the corresponding spacetime diagram for the ingoing and outgoing light rays. Here $\hat{x}$, $\hat{a}_{in}$ and $\hat{a}_{out}$ denote the oscillator position, ingoing and outgoing fields, ω_m, κ_m stand for oscillator frequency and decay rate, $\hat{a}$, κ and L denote intracavity optical mode, cavity bandwidth and length, respectively. We assume bad cavity limit when $\kappa \gg \omega_m$ and thus the dynamics of $\hat{a}$ can be considered following the ingoing light adiabatically. For clarity, we intentionally place $\hat{a}_{in}$ and $\hat{a}_{out}$ on different sides of the oscillator world line. The inclined lines represent the light rays. Up to some instant we are concerned with ($t = 0$), the optical fields entering later are out of causal contact and thus irrelevant.

This paper is organised as follows: in Sec. II, we set our model of optomechanical system and derive the dynamics thereof; in Sec. III, we consider a conditional dynamics of Gaussian mechanical states resulting from continuous monitoring of the outgoing light; in Sec. IV an entanglement between the outgoing light and mechanical oscillations of the cavity mirror is studied in detail; Sec. V is devoted to the use of the optomechanical entanglement for experimental demonstration of the quantum state steering; Sec. VI contains some summarising remarks and concludes this paper.

II. OPTOMECHANICAL SYSTEM AND CONTINUOUS MEASUREMENT

We start by considering a dynamics of a linear optomechanical device presented in Fig. 1 which has been extensively studied [12, 18–20]; its linearised Hamiltonian reads:

$$\hat{\mathcal{H}} = \hat{p}^2/(2m) + m\omega_m^2\hat{x}^2/2 + \hat{\mathcal{H}}_{\kappa_m} + \hbar\Delta\hat{a}^\dagger\hat{a} + \hbar g\hat{x}(\hat{a}^\dagger + \hat{a})$$
$$+ i\hbar\sqrt{\kappa}(\hat{a}_{\text{ext}}\hat{a}^\dagger - \hat{a}_{\text{ext}}^\dagger\hat{a}). \tag{1}$$

Here ω_m is the mechanical resonant frequency; $\Delta = \omega_c - \omega_l$ is cavity detuning, i.e., difference between the cavity resonant frequency ω_c and the laser frequency ω_l; $\hat{\mathcal{H}}_{\kappa_m}$ summarises the fluctuation-dissipation mechanism for the mechanical oscillator; the fifth term is the optomechanical interaction term with $g \equiv \bar{a}\omega_c/L$ quantifying the coupling strength, $\bar{a}$ the steady-state amplitude of the cavity mode and L the cavity length; the last term describes the coupling between the cavity mode and external continuous optical field $\hat{a}_{\text{ext}}$ with $[\hat{a}_{\text{ext}}(t), \hat{a}_{\text{ext}}^\dagger(t')] = \delta(t - t')$ in the Makovian limit and κ is the coupling rate which is also the cavity bandwidth.

From Hamiltonian (1), one can obtain the following set of linear Heisenberg equations of motion

$$m[\ddot{\hat{x}}(t) + \kappa_m\dot{\hat{x}}(t) + \omega_m^2\hat{x}(t)] = \hat{F}_{\text{rp}}(t) + \hat{F}_{\text{th}}(t), \tag{2}$$

$$\dot{\hat{a}}(t) + (\kappa/2 + i\Delta)\hat{a}(t) = -ig\hat{x}(t) + \sqrt{\kappa}\hat{a}_{\text{in}}(t), \tag{3}$$

and the input-output relation

$$\hat{a}_{\text{out}}(t) = -\hat{a}_{\text{in}}(t) + \sqrt{\kappa}\hat{a}(t), \tag{4}$$

where $\hat{a}_{\text{in}} \equiv \hat{a}_{\text{ext}}(t_-)$ (in-going) and $\hat{a}_{\text{out}} \equiv \hat{a}_{\text{ext}}(t_+)$ (out-going) are input and output operators in the standard input-output formalism [21], and $\hat{F}_{\text{rp}} \equiv -\hbar g(\hat{a} + \hat{a}^\dagger)$ is the quantum radiation pressure force and $\hat{F}_{\text{th}}$ is the thermal fluctuation force associated with the mechanical damping. Output field $\hat{a}_{\text{out}}$ can be measured with a homodyne detection scheme, from which we can infer the mechanical motion and thus the quantum state of the oscillator. By adjusting the local oscillator phase, one can measure any θ-quadrature: $\hat{b}_\theta = \hat{b}_1\sin\theta + \hat{b}_2\cos\theta$, which is a linear combination of the output amplitude quadrature $\hat{b}_1 \equiv \frac{1}{\sqrt{2}}(\hat{a}_{\text{out}} + \hat{a}_{\text{out}}^\dagger)$ and phase quadrature $\hat{b}_2 \equiv \frac{1}{\sqrt{2}i}(\hat{a}_{\text{out}} - \hat{a}_{\text{out}}^\dagger)$. After incorporating non-unity photodetection efficiency η, the measurement output at time t is given by

$$\hat{y}_\theta(t) = \sqrt{\eta}[\hat{b}_1(t)\sin\theta + \hat{b}_2(t)\cos\theta] + \sqrt{1-\eta}\,\hat{n}_\theta(t), \tag{5}$$

where $\hat{n}_\theta$ is the vacuum noise associated with the photodetection loss and is uncorrelated with $\hat{a}_{\text{in}}$. Note that θ can be a function of time, when the local oscillator phase is adjusted during the measurement; in this way a different optical quadrature (but only one) is measured at each moment of time.

Large cavity bandwidth and strong measurement limit.— The particular scenario that allows for concise form expressions and at the same time represents all the physics is theone when the cavity bandwidth is large and the optomechanical coupling rate is strong — a strong measurement, compared to the mechanical resonant frequency ω_m. In this case, the
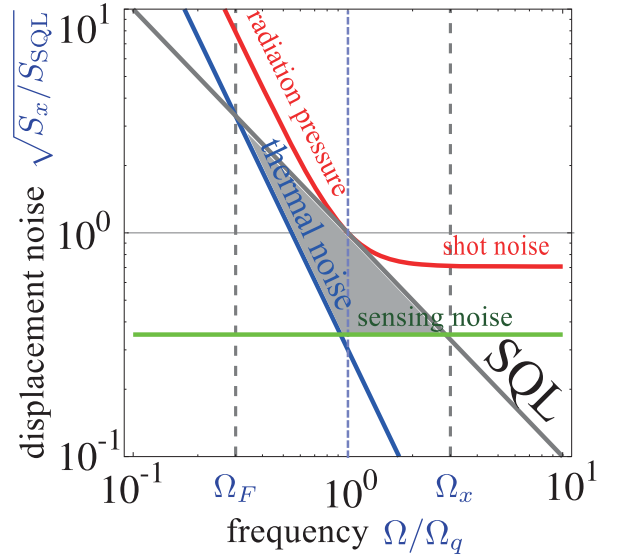

FIG. 2. The displacement noise spectrum of an optomechanical device and the characteristic frequencies of the force noise Ω_F, the quantum noise Ω_q, and the sensing noise Ω_x referring to the Standard Quantum Limit (SQL) in the strong measurement, bad-cavity limit, i.e. when $\kappa \gg \Omega_q \gg \omega_m$.

cavity mode can be adiabatically eliminated, and the mechanical resonant frequency ω_m ignored (for general scenarios, the formalism here still applies but the analytical results become quite complicated). Correspondingly, equations of motion for the oscillator read reads [cf. Eqs. (2) and (3)]:

$$m\ddot{\hat{x}}(t) = \hat{F}_{\text{rp}}(t) + \hat{F}_{\text{th}}(t) = -\alpha\hat{a}_1(t) + \hat{F}_{\text{th}}(t), \tag{6}$$

with $\hat{a}_1 \equiv \frac{1}{\sqrt{2}}(\hat{a}_{\text{in}} + \hat{a}_{\text{in}}^\dagger)$ the amplitude quadrature of the input field. The output amplitude quadrature $\hat{y}_1$ and phase quadrature $\hat{y}_2$ are given by [cf. Eqs. (4) and (5)]:

$$\hat{y}_1(t) = \sqrt{\eta}\,\hat{a}_1(t) + \sqrt{1-\eta}\,\hat{n}_1(t), \tag{7}$$

$$\hat{y}_2(t) = \sqrt{\eta}[\hat{a}_2(t) + (\alpha/\hbar)\hat{x}(t)] + \sqrt{1-\eta}\,\hat{n}_2(t), \tag{8}$$

where $\hat{a}_2 \equiv \frac{1}{\sqrt{2}i}(\hat{a}_{\text{in}} - \hat{a}_{\text{in}}^\dagger)$ is the phase quadrature of the input field, and additionally we have introduced an effective coupling constant (measurement strength) $\alpha \equiv \sqrt{8/\kappa}\,\hbar g$.

In this special case, all the noise sources are Markovian and thus can be characterised by single values of their spectral densities. However, it is instructive to introduce characteristic frequencies thereof, where displacement spectrums intersect the standard quantum limit (SQL) as a benchmark: $\Omega_F \equiv [2m\kappa_m k_B T/(\hbar m)]^{1/2}$, $\Omega_q \equiv [\alpha^2/(\hbar m)]^{1/2}$, and $\Omega_x \equiv \Omega_q[2\eta/(1-\eta)]^{1/2}$. In Fig. 2, we plot these noise sources in the strong measurement limit, when quantum fluctuations of light dominate over all other noise sources in some frequency band, set by the values of Ω_F and Ω_x. This is the general requirement one has to satisfy to be able to see quantum correlations, or use them for manipulations with mechanical quantum states [10, 22].

III.   CONDITIONAL QUANTUM STATE.

Now suppose we perform homodyne detection during $-\tau \leq t \leq 0$, obtaining a data string:

$$\boldsymbol{y}_\theta = \{y_\theta(-\tau), y_\theta(-\tau + dt), \cdots, y_\theta(-dt), y_\theta(0)\} \quad (9)$$

with $dt = \tau/(N-1)$ being the time increment and N the number of data points. We can then infer the quantum state of mechanical oscillator at $t = 0$ conditional on these measurement data, obtaining the so-called conditional quantum state. The standard way to obtain the conditional state is to use data to drive the stochastic master equation [23–27]. Here we use a different approach by using the Wigner quasi-probability distributions, deriving the conditional quantum state in a way similar to classical Bayesian statistics, in the same spirit as the approach applied in Ref. [22]; this allows us to more straightforwardly treat non-Markovianity, e.g., due to a small cavity bandwidth and colored classical noises. Our approach takes the advantage of the following facts:

$$[\hat{y}_\theta(t), \hat{y}_\theta(t')] = [\hat{x}(0), \hat{y}_\theta(t)] = [\hat{p}(0), \hat{y}_\theta(t)] = 0 \quad (10)$$

$\forall t, t' \in [-\tau, 0]$, which is a consequence of the general features of linear continuous quantum measurements [28]. We can therefore treat $\hat{y}_\theta(t)$ almost as classical quantities and ignore their time-ordering in deriving the following joint Wigner function of the oscillator and the continuous optical field:

$$W(\boldsymbol{x}, \boldsymbol{y}_\theta) = \text{Tr}[\hat{\rho}(-\tau)\delta^{(2)}(\hat{\boldsymbol{x}} - \boldsymbol{x})\delta^{(N)}(\hat{\boldsymbol{y}}_\theta - \boldsymbol{y}_\theta)]. \quad (11)$$

Here we have only included the marginal distribution for the optical quadrature $\hat{\boldsymbol{y}}_\theta$ of interests, instead of the entire optical phase space; $\hat{\boldsymbol{x}} \equiv (\hat{x}(0), \hat{p}(0))$ and $\boldsymbol{x}$ is a c-number vector, similar for $\boldsymbol{y}_\theta$; $\hat{\rho}(-\tau)$ is the initial joint density matrix

$$\hat{\rho}(-\tau) = \hat{\rho}_m^{\text{th}} \otimes |\mathbf{0}\rangle\langle\mathbf{0}| \quad (12)$$

with $\hat{\rho}_m^{\text{th}}$ the thermal state of the oscillator and $|\mathbf{0}\rangle$ the vacuum state for the optical field—the coherent amplitude of the laser has been absorbed into the optomechanical coupling constant g. Since $\hat{x}(0)$ and $\hat{p}(0)$ do not commute we have to explicitly define $\delta^{(2)}(\hat{\boldsymbol{x}} - \boldsymbol{x}) = \int d^2\boldsymbol{\xi} e^{-i\boldsymbol{\xi}\cdot(\hat{\boldsymbol{x}}-\boldsymbol{x})}$. Similar to classical Bayesian statistics, the Wigner function for the conditional quantum state of the mechanical oscillator at $t = 0$ reads:

$$W_m(\boldsymbol{x}|\boldsymbol{y}_\theta) = W(\boldsymbol{x}, \boldsymbol{y}_\theta)/W(\boldsymbol{y}_\theta). \quad (13)$$

Since we consider only Gaussian quantum states, the joint Wigner function can thus be formally written as:

$$W(\boldsymbol{x}, \boldsymbol{y}_\theta) = c_0 \exp\left[-\frac{1}{2}(\boldsymbol{x}, \boldsymbol{y}_\theta)\mathbf{V}_\theta^{-1}(\boldsymbol{x}, \boldsymbol{y}_\theta)^{\text{T}}\right], \quad (14)$$

where c_0 is the normalization factor and superscript $^\text{T}$ denotes transpose. Elements of the covariance matrix $\mathbf{V}_\theta$ are given by

$$\mathbf{V}_\theta^{jk} = \langle\hat{\boldsymbol{X}}_j\hat{\boldsymbol{X}}_k\rangle_{\text{sym}} \equiv \text{Tr}[\hat{\rho}(-\tau)(\hat{\boldsymbol{X}}_j\hat{\boldsymbol{X}}_k + \hat{\boldsymbol{X}}_k\hat{\boldsymbol{X}}_j)]/2 \quad (15)$$

with $\hat{\boldsymbol{X}} \equiv (\hat{\boldsymbol{x}}, \hat{\boldsymbol{y}}_\theta)$. We separate components of the oscillator and the optical field, and rewrite the covariance matrix $\mathbf{V}$ as:

$$\mathbf{V}_\theta = \begin{bmatrix} \mathbf{A} & \mathbf{C}_\theta^{\text{T}} \\ \mathbf{C}_\theta & \mathbf{B}_\theta \end{bmatrix} \equiv \begin{bmatrix} \mathbf{A} & \mathbf{C}^{\text{T}}\boldsymbol{u}_\theta^{\text{T}} \\ \boldsymbol{u}_\theta\mathbf{C} & \boldsymbol{u}_\theta\mathbf{B}\boldsymbol{u}_\theta^{\text{T}} \end{bmatrix}. \quad (16)$$

Here $\mathbf{A}$ is a 2×2 covariance matrix for the mechanical oscillator position $\hat{x}(0)$ and momentum $\hat{p}(0)$; $\mathbf{B}$ is a $2N \times 2N$ covariance matrix for two quadratures $\hat{\boldsymbol{y}}_1 \equiv \hat{\boldsymbol{y}}_{\theta=\pi/2}$ and $\hat{\boldsymbol{y}}_2 \equiv \hat{\boldsymbol{y}}_{\theta=0}$ of the optical field; $\boldsymbol{u}_\theta = (\sin\boldsymbol{\theta}, \cos\boldsymbol{\theta})$ is a $N \times 2N$ matrix and $\sin\boldsymbol{\theta} \equiv \text{diag}[\sin\theta(-\tau), \cdots, \sin\theta(0)]$—a diagonal matrix with elements being quadrature angle at different times; $\mathbf{C}$ is a $2N \times 2$ matrix describing the correlation between $(\hat{\boldsymbol{y}}_1, \hat{\boldsymbol{y}}_2)$ and $(\hat{x}(0), \hat{p}(0))$. Combining Eqs. (13) and (16), we obtain:

$$W_m(\boldsymbol{x}|\boldsymbol{y}_\theta) = \frac{1}{\pi\hbar}\exp\left[-\frac{1}{2}(\boldsymbol{x} - \boldsymbol{x}^{|\theta})\mathbf{V}_m^{|\theta-1}(\boldsymbol{x} - \boldsymbol{x}^{|\theta})^{\text{T}}\right], \quad (17)$$

where the conditional mean $\boldsymbol{x}^{|\theta}$ and covariance matrix $\mathbf{V}_m^{|\theta}$ are

$$\boldsymbol{x}^{|\theta} = \mathbf{C}_\theta^{\text{T}}\mathbf{B}_\theta^{-1}\boldsymbol{y}_\theta^{\text{T}}, \quad \mathbf{V}_m^{|\theta} = \mathbf{A} - \mathbf{C}_\theta^{\text{T}}\mathbf{B}_\theta^{-1}\mathbf{C}_\theta. \quad (18)$$

Note that the two rows of the $2N \times 2$ matrix, $\mathbf{C}_\theta^{\text{T}}\mathbf{B}_\theta^{-1}$, which we shall refer to as $\boldsymbol{K}_x$ (the first row) and $\boldsymbol{K}_p$ (the second row), are also the optimal filters that predict $\hat{x}(0)$ and $\hat{p}(0)$ with minimum errors, $\langle[\hat{x}(0) - \boldsymbol{K}_x\hat{\boldsymbol{y}}_\theta^{\text{T}}]^2\rangle$ and $\langle[\hat{p}(0) - \boldsymbol{K}_p\hat{\boldsymbol{y}}_\theta^{\text{T}}]^2\rangle$, respectively. The above results for the conditional mean and variance are formally identical to those obtained by classical optimal filtering.

Continuous-time limit.—To properly describe the actual continuous measurement process, we take the continuous-time limit with $dt \to 0$, and we have $N \to \infty$. The matrices indexed by time become functions of time, while matrix products involving summing over time become integrals. In particular, the central problem of calculating $\boldsymbol{K} = \mathbf{C}^{\text{T}}\mathbf{B}^{-1}$ becomes solving an integral equation for $\boldsymbol{K}$:

$$\int_{-\tau}^0 dt' \mathbf{B}(t, t')\boldsymbol{K}(t') = \mathbf{C}^{\text{T}}(t). \quad (19)$$

More specifically, $\mathbf{B}(t, t')$ now becomes a 2×2 matrix with elements being the two-time correlation functions between optical quadratures $\hat{y}_1(t)$ and $\hat{y}_2(t')$; $\mathbf{C}(t)$'s elements are correlation functions between $(\hat{y}_1(t), \hat{y}_2(t'))$ and $(\hat{x}(0), \hat{p}(0))$. These correlation functions can in turn be obtained by solving Heisenberg equations of motion [cf. Eqs. (2-5)] and expressing $\hat{x}(0)$, $\hat{p}(0)$, $\hat{y}_1(t)$, and $\hat{y}_2(t)$ in terms of $\hat{a}_{\text{in}}(t)$, $\hat{n}(t)$ and $\hat{F}_{\text{th}}(t)$, for which we have $\langle\hat{a}_{\text{in}}(t)\hat{a}_{\text{in}}^\dagger(t')\rangle_{\text{sym}} = \delta(t - t')/2$, $\langle\hat{n}(t)\hat{n}(t')\rangle_{\text{sym}} = \delta(t - t')/2$ and $\langle\hat{F}_{\text{th}}(t)\hat{F}_{\text{th}}(t')\rangle_{\text{sym}} = 2m\kappa_m k_B T\delta(t - t')$ given the initial state $\hat{\rho}(-\tau)$ shown in Eq. (12). The above integral equation is generally difficult to solve analytically if τ is finite. Since usually we are not interested in the transient dynamics, we can extend $-\tau$ to $-\infty$, which physically corresponds to waiting long enough till the mechanical oscillator approaches a steady state, and then start state preparation. In this case, Eq. (19) can be solved analytical using the Wiener-Hopf method of which the detail is shown in the Appendix A.

IV. OPTOMECHANICAL UNIVERSAL ENTANGLEMENT

Now we can consider a problem of entanglement between the mechanical oscillator and the outgoing light fields. Effectively, it is equivalent to bipartite enatanglement of a single particle with $N \to \infty$ other particles. According to Refs. [29, 30], in order for one particle and a joint system of arbitrarily large N particles to be separable, a necessary and sufficient condition is that partially transposed density matrix $\rho_{1|N}^{\mathbf{T_1}}$ (with respect to the first particle) should be *positive semidefinite*, i.e. $\rho_{1|N}^{\mathbf{T_1}} \geq 0$. In the phase space of continuous Gaussian variables, this reduces to the *Uncertainty Principle*

$$\mathbf{V}_{\mathrm{pt}} + i\boldsymbol{\Sigma} \geq 0, \quad \boldsymbol{\Sigma} = \bigoplus_{k=1}^{N+1} \sigma_k \text{ where } \sigma_k = \begin{bmatrix} 0 & 1 \\ -1 & 0 \end{bmatrix} \quad (20)$$

Here we introduced a complete covariance matrix of the optomechanical system $\mathbf{V} \in \mathbb{R}^{(2N+2,2N+2)}$ as:

$$\mathbf{V} \equiv \begin{bmatrix} \mathbf{A} & \mathbf{C}^{\mathbf{T}} \\ \mathbf{C} & \mathbf{B} \end{bmatrix} \quad (21)$$

and its partial transpose $\mathbf{V}_{\mathrm{pt}} = \mathbf{T}_1 \mathbf{V} \mathbf{T}_1$, where transformation $\mathbf{T}_1 = \mathrm{Diag}[1, -1] \oplus \mathbf{I}_{2N}$, with $\mathbf{I}_{2N} \in \mathbb{R}^{(2N,2N)}$ identity matrix, performs a time inversion operation for a mechanical part of the system: $\mathbf{V}_{\mathrm{pt}} = \mathbf{V}|_{\hat{p}(0) \to -\hat{p}(0)}$ which is equivalent to transpose of mechanical sub-matrix in joint optomechanical density matrix $\rho_{1|N}$ [30].

According to the Williamson theorem, there exists a symplectic transformation $\mathbf{S} \in S_{p(2N+2,\mathbb{R})}$ such that $\mathbf{S}^{\mathbf{T}} \mathbf{V}_{\mathrm{pt}} \mathbf{S} = \bigoplus_{k=1}^{N+1} \mathrm{Diag}[\lambda_k, \lambda_k]$. Using the fact that $\mathbf{S}^{\mathbf{T}} \boldsymbol{\Sigma} \mathbf{S} = \boldsymbol{\Sigma}$, the above *Uncertainty Principle* reads $\lambda_k \geq 1$. If this fails to be the case, i.e. $\exists \lambda_k < 1$, the states are entangled. The amount of entanglement can be quantified by the logarithmic negativity $E_{\mathcal{N}}$ [31] and

$$E_{\mathcal{N}} \equiv \max[-\textstyle\sum_k \ln \lambda_k, 0] \quad \text{for } k : \lambda_k < 1. \quad (22)$$

Going for continuous time limit $N \to \infty$, one can find λ_k by solving eigenvalue problem [31]:

$$\mathbf{V}_{\mathrm{pt}} \mathbf{v} = i\lambda \boldsymbol{\Sigma} \mathbf{v}, \quad (23)$$

where $\mathbf{v} \equiv [\alpha_0, \beta_0, |\alpha\rangle, |\beta\rangle]^{\mathbf{T}}$ with $|f\rangle$ denoting function of time which belongs to $\mathscr{L}^2[-\infty, 0]$. Due to uniqueness of $|\alpha\rangle$ and $|\beta\rangle$ in terms of α_0 and β_0 for any $\lambda < 1$ (non-singular), Eq. (23) leads to the following characteristic polynomial equation

$$\det[\mathbf{A} + i\lambda \sigma_k - \mathbf{C}^{\mathbf{T}}(i\lambda \sigma_k + \mathbf{B})^{-1}\mathbf{C}] = 0 \quad (24)$$

Inversion of matrix $i\lambda \sigma_k + \mathbf{B}$ in continuous limit can be done using the same Wiener-Hopf method discussed above and presented in Appendix A. Solution shows, there is always one eigenvalue λ that is smaller than one and it only depends on the ratio between Ω_q and Ω_F, which clearly indicates the universality of the quantum entanglement. In Fig. 3, the corresponding logarithmic negativity (c.f. Eq. (22)) is shown as a function of Ω_q/Ω_F. For a high-Q oscillator
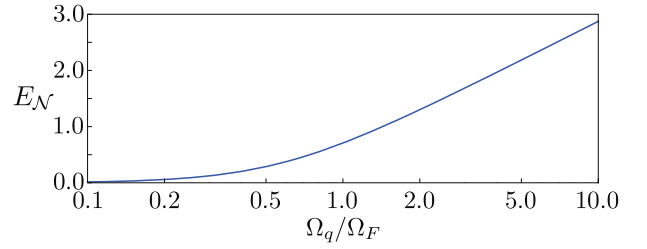

FIG. 3. Logarithmic negativity $E_{\mathcal{N}}$ as a function of the ratio Ω_q/Ω_F. A mechanical quality factor $Q_m = 10^3$ is chosen.

$Q_m \equiv \omega_m/(2\kappa_m) \gg 1$, up to the leading order of $1/Q_m$, a very elegant expression for $E_{\mathcal{N}}$ is derived and it is

$$E_{\mathcal{N}} = (1/2)\ln[1 + (25/8)\Omega_q^2/\Omega_F^2]. \quad (25)$$

This expression clearly demonstrates that optomechanical entanglement persists at any temperature, as its measuer, the logarithmic negativity, depends only on the ratio of measurement strength Ω_q and thermal decoherence rate Ω_F. In the previous works on optomechanical entanglement [6, 8, 11], it depends solely on decoherence rate Ω_F. However, as we showed in [12, 13], this is a consequence of disregarding the information that was carried out by the outgoing light and considering only the entanglement between the intracavity optical mode and the oscillator. When the continuum of the modes leaving the cavity is properly accounted for, optomechanical entanglement turns out to be universal.

Let us now consider how long can this entanglement survive. After turning off the optomechanical coupling at $t = 0$, the mechanical oscillator freely evolves for a finite duration τ, driven only by thermal noise. Due to thermal decoherence, entanglement will gradually vanish. Mathematically, the symplectic eigenvalue will become larger than unity when τ is larger than the survival time τ_s. By replacing $[\hat{x}(0), \hat{p}(0)]$ with $[\hat{x}(\tau), \hat{p}(\tau)]$ and making similar analysis, up to the leading order of $1/Q_m$, τ_s satisfies a transcendental equation: $4\Omega_F^4 \theta_s^2 - (2\Omega_F^2 + \Omega_q^2)^2 \sin^2 \theta_s - 25 \omega_m^4 = 0$, with $\theta_s \equiv \omega_m \tau_s$. In the case of $\Omega_q > \Omega_F \gg \omega_m$, the oscillating term can be neglected, leading to

$$\theta_s = (5/2)(\omega_m/\Omega_F)^2 = 5 Q_m/(2\bar{n}_{\mathrm{th}} + 1), \quad (26)$$

where we have defined the thermal occupation number $\bar{n}_{\mathrm{th}}$ through $k_B T/(\hbar \omega_m) = \bar{n}_{\mathrm{th}} + (1/2)$. Therefore, in this case if Q_m is larger than n_{th}, the entanglement will be able to survive longer than one oscillation period. Since $Q_m > n_{\mathrm{th}}$ is also the requirement that the thermal noise induces a momentum diffusion smaller than its zero-point uncertainty [28], this condition is what we intuitively expect. In the strong measurement case with $\Omega_q \gg \Omega_F$, the transcendental equation can be solved numerically, showing that $\theta_s > 1$ is always valid and the entanglement can survive at least up to one oscillation period.

It is evident from the above that optomechanical entanglement is a powerful resource for recovering macroscopic quantum correlations. In the next section we consider how it can be used to demonstrate "steering" of mechanical quantum state by a different choice of measured quadrature of light.

V.   QUANTUM-STATE STEERING.

Optomechanical steering concept. — According to quantum mechanics, position and momentum of a mechanical oscillator satisfy the Heisenberg uncertainty principle, which reads:

$$\Delta X_{\phi_1} \Delta X_{\phi_2} \geq |\sin(\phi_1 - \phi_2)|, \quad \forall \phi_1, \phi_2 \qquad (27)$$

where $\hat{X}_\phi \equiv (\hat{x}/\Delta x_q)\sin\phi + (\hat{p}/\Delta p_q)\cos\phi$, with Δx_q and Δp_q zero-point uncertainties in position and momentum, are quadratures of the mechanical oscillator. Since the mechanical oscillator is interacting and establishing entanglement with a continuous optical field, one can collapse it into desired quantum state simply measuring continuously the outgoing light with time-dependent homodyne angle $\theta(t)$ that defines which optical quadrature is measured at time t. Suppose the measurement lasts from $-\tau$ up to 0, the final conditional state of the oscillator, written as $|\psi_m^{|\theta}(0)\rangle$, will depend on how we make the homodyne detection due to entanglement. For two different measurement strategies with $\theta_1(t)$ and $\theta_2(t)$, respectively, in general we have two different final conditional states: $|\psi_m^{|\theta_1}(0)\rangle \neq |\psi_m^{|\theta_2}(0)\rangle$. If the quadratures are properly chosen, we may have, as illustrated in Fig. 4:

$$\Delta X_{\phi_1}^{|\theta_1} \Delta X_{\phi_2}^{|\theta_2} < |\sin(\phi_1 - \phi_2)|, \qquad (28)$$

where $\Delta X_{\phi_k}^{|\theta_k} \equiv \langle(\hat{X}_{\phi_k} - \langle\hat{X}_{\phi_k}\rangle)^2\rangle^{1/2}$ with $\langle\cdot\rangle \equiv \langle\psi_m^{|\theta_k}|\cdot|\psi_m^{|\theta_k}\rangle$.

In other words, if in the first strategy, the observer tries to predict quadrature X_{ϕ_1} of the mechanical oscillator, while in the second strategy, the observer tries to predict X_{ϕ_2}, then the two predictions have an error product that is *lower* than Heisenberg Uncertainty. The possible way to do it is summarised in Fig. 5.

In ideal linear quantum measurement processes, both conditional states will be pure, and for any pairs of distinctive θ_1 and θ_2, inequality (28) will almost always exist for some set of ϕ_1 and ϕ_2—although this idealised steerability may be influenced by practical imperfections, such as thermal noise.
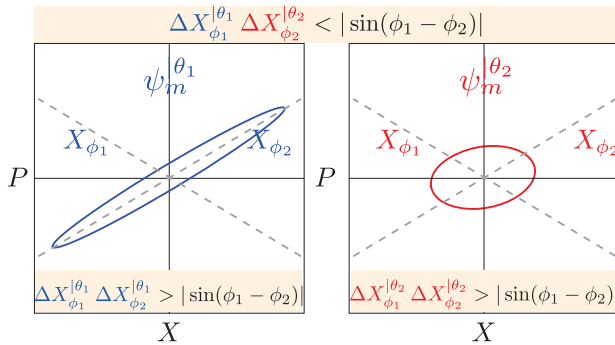

FIG. 4.   (color online) Two different quantum states (projection of their Wigner functions on phase space) of a mechanical oscillator, conditional on two different strategies for measuring the optical quadrature: one at $\theta_1(t)$ (left) and the other at $\theta_2(t)$ (right).
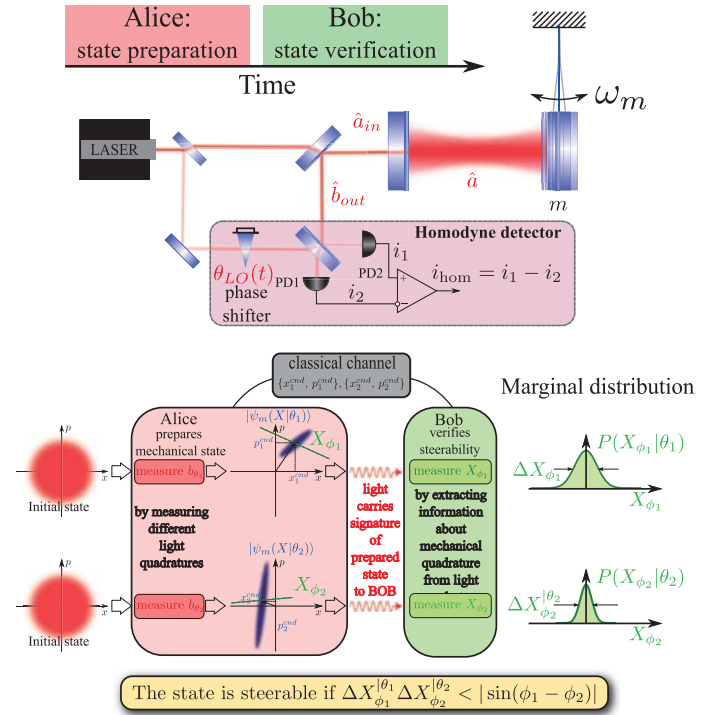

FIG. 5. Scheme of possible experimental setup (upper panel) and the time chart of the experiment demonstrating optomechanical steering (lower panel). Here Alice, using two different measurement strategies $\theta_{1,2}(t)$ (two time-dependent homodyne angles), prepares many copies of two conditional states of the mechanical oscillator, $|\psi_m^{|\theta_1}(0)\rangle$ and $|\psi_m^{|\theta_2}(0)\rangle$, and passes the prepared states to Bob, also providing him with sets of conditional estimates of position ($x^{cnd}(0)$) and momentum ($p^{cnd}(0)$) of the oscillator at time $t = 0$, which she derives at each instance of state preparation. Bob, using the same setup, measures from $t = 0$ onwards, two different mechanical quadratures of the oscillator, X_{ϕ_1} and X_{ϕ_2}, and reconstructs marginal probability distributions for these two quadratures. By calculating variances $\Delta X_{\phi_1}^{|\theta_1}$ and $\Delta X_{\phi_2}^{|\theta_2}$, he tests if Alice has succeeded in steering the mechanical state of the oscillator.

In view of Eq.(28), we introduce a figure of merit to quantify steerability,

$$\mathscr{S} \equiv -\min_{\phi_1, \phi_2, \theta_1, \theta_2} \left\{ \ln \frac{\Delta X_{\phi_1}^{|\theta_1} \Delta X_{\phi_2}^{|\theta_2}}{|\sin(\phi_1 - \phi_2)|} \right\}. \qquad (29)$$

with minimum obtained by comparing all possible sets of $\{\phi_1, \theta_1(t), \phi_2, \theta_2(t)\}$ ($t \in [-\tau, 0]$)—an optimal time-dependent homodyne detection is needed to achieve the lower bound. The quantum state is steerable when $\mathscr{S} > 0$, which will be proved to be equivalent to the formal criterion obtained by Wiseman for Gaussian entangled states [14].

As we will show in the discussion that follows, for linear optomechanical devices, when the quantum radiation pressure dominates strongly over thermal fluctuations, steerability only depends on the photodetector efficiency η of time-dependent

homodyne detections:

$$\mathscr{S} \approx \frac{1}{2}\left[\ln \eta - \ln(1 - \eta)\right], \tag{30}$$

which will be positive as long as $\eta > 50\%$, which coincides with the ideal limit shown by Wiseman and Gambetta [14]. Interestingly, such quantum steerability is intimately related to the state tomography accuracy in the protocol suggested by Miao *et al.* [32], in which an optimal time-dependent homodyne detection scheme is used to probe the quantum state of a mechanical oscillator with Gaussian-distributed joint position and momentum error less than Heisenberg uncertainty. More explicitly, we will show, for the same optomechanical device,

$$\mathscr{S} = -\ln\left[2\sqrt{\det \mathbf{V}_v}/\hbar\right], \tag{31}$$

where $\mathbf{V}_v$ is the covariance matrix for the tomography error.

Theory of optomechanical steering. — We can now understand the quantum-state steering from a more quantitative way. From Eq. (18), we learned that the conditional variance of the oscillator state $\mathbf{V}_m^{|\theta}$ directly depends on the optical quadrature θ that we choose to measure. To calculate the steerability figure of merit $\mathscr{S}$ [cf. Eq. (29)], we need to find the time-dependent quadrature phase $\theta(t)$ that minimise the conditional variance $\Delta X_\phi^{|\theta}$ of a given mechanical quadrature $\hat{X}_\phi = \boldsymbol{v}_\phi \hat{\mathbf{x}}^{\mathrm{T}}$ with vector $\boldsymbol{v}_\phi \equiv (\sin\phi/\Delta x_q, \cos\phi/\Delta p_q)$. Using the fact that

$$\min_\theta (\Delta X_\phi^{|\theta})^2 = \min_{\theta,\boldsymbol{K}} \langle \boldsymbol{v}_\phi \hat{\mathbf{x}}^{\mathrm{T}} - \boldsymbol{K}\hat{\mathbf{y}}_\theta^{\mathrm{T}}\rangle^2$$
$$= \min_{\boldsymbol{K}_1,\boldsymbol{K}_2} \langle \boldsymbol{v}_\phi \hat{\mathbf{x}}^{\mathrm{T}} - \boldsymbol{K}_1 \hat{\mathbf{y}}_1^{\mathrm{T}} - \boldsymbol{K}_2 \hat{\mathbf{y}}_2^{\mathrm{T}}\rangle^2 \tag{32}$$

with $\boldsymbol{K}_1 \equiv \boldsymbol{K}\sin\boldsymbol{\theta}$ and $\boldsymbol{K}_2 \equiv \boldsymbol{K}\cos\boldsymbol{\theta}$, we obtain the minimum

$$(\Delta X_\phi^{|\theta})^2_{\min} = \boldsymbol{v}_\phi (\mathbf{A} - \mathbf{C}^{\mathrm{T}}\mathbf{B}^{-1}\mathbf{C})\boldsymbol{v}_\phi^{\mathrm{T}}, \tag{33}$$

and $\theta(t_k)$ at $t = -\tau + k\,\mathrm{d}t$ is given by:

$$\theta(t_k) = \arctan\left[(\boldsymbol{v}_\phi \mathbf{C}^{\mathrm{T}}\mathbf{B}^{-1})_k / (\boldsymbol{v}_\phi \mathbf{C}^{\mathrm{T}}\mathbf{B}^{-1})_{N+k}\right]. \tag{34}$$

Since $(\Delta X_\phi^{|\theta})^2_{\min}$ is in a quadratic form of $\boldsymbol{v}_\phi$, we obtain:

$$\mathscr{S} = -\ln\left[2\sqrt{\det \mathbf{V}_s}/\hbar\right], \quad \mathbf{V}_s \equiv \mathbf{A} - \mathbf{C}^{\mathrm{T}}\mathbf{B}^{-1}\mathbf{C}. \tag{35}$$

This means quantum state of the oscillator is not steerable— $\mathscr{S} < 0$, if $\mathbf{V}_s$ is Heisenberg limited—$\sqrt{\det \mathbf{V}_s} > \hbar/2$.

Such a definition of steerability is in accord with the criterion by Wiseman *et al.* [14], more specifically, shown in their Eq. (17), which says that quantum state of the oscillator *cannot* be steered by the optical field, if we have

$$\begin{bmatrix} \mathbf{A} & \mathbf{C}^{\mathrm{T}} \\ \mathbf{C} & \mathbf{B} \end{bmatrix} + i\boldsymbol{\Sigma}_m \oplus \mathbf{0}_o > 0, \tag{36}$$

where $\boldsymbol{\Sigma}_m \equiv \sigma_k$ is the 2×2 symplectic matrix for the oscillator, and $\mathbf{0}_o$ is a null $2N \times 2N$ matrix for the optical field. Since the

covariance matrix $\mathbf{B}$ for the optical field is positive definite, namely, $\mathbf{B} > 0$, the above condition requires that the Schur's complement of $\mathbf{A}$ be positive definite:

$$\mathbf{A} - \mathbf{C}^{\mathrm{T}}\mathbf{B}^{-1}\mathbf{C} + i\boldsymbol{\Sigma}_m = \mathbf{V}_s + i\boldsymbol{\Sigma}_m > 0, \tag{37}$$

which is equivalent to requiring that $\mathbf{V}_s$ is Heisenberg limited, i.e.,

$$\mathscr{S} = -\ln\left[2\sqrt{\det \mathbf{V}_s}/\hbar\right] < 0. \tag{38}$$

Large cavity bandwidth and strong measurement limit. — Using the equations (7) and (8) and the definitions of Ω_q, Ω_x and Ω_F thereafter, we can easily obtain those correlation functions in the integral equation shown in Eq. (19). Using Wiener-Hopf method of Appendix A, one can easily solve it and get the following expression for $\mathbf{V}_s$:

$$\mathbf{V}_s = \frac{\hbar\zeta_F}{\sqrt{2}\,\eta}\begin{bmatrix} 2^{\frac{1}{4}}\sqrt{\alpha^2/(\zeta_F\hbar m)} & 1 \\ 1 & 2^{\frac{3}{4}}\sqrt{\zeta_F\hbar m/\alpha^2} \end{bmatrix}, \tag{39}$$

where the characteristic constant ζ_F is defined as:

$$\zeta_F \equiv \left[\frac{\eta}{2}\left(1 - \eta + \frac{4m\kappa_m k_B T}{\alpha^2}\right)\right]^{1/2}. \tag{40}$$

Correspondingly, we obtain the steerability [cf. Eq. (35)]:

$$\mathscr{S} = -\ln\left(\sqrt{2}\,\zeta_F/\eta\right). \tag{41}$$

For a strong measurement, the quantum radiation pressure dominates over the thermal fluctuation force, and we have $S_F^{\mathrm{rp}} = \alpha^2 \gg S_F^{\mathrm{th}} = 4m\kappa_m k_B T$, with S_F^{rp} and S_F^{th} being the single-sided spectra density—twice the Fourier transform of two-time correlation function. This leads to $\zeta_F \approx \sqrt{\eta(1-\eta)/2}$ and $\mathscr{S} \approx \frac{1}{2}\ln[\eta/(1-\eta)]$, as shown in Eq. (30).

Connection between steering and quantum tomography. — Interestingly, such quantum-state steering is closely related to the quantum tomography protocol discussed in Ref. [32], where an optimal time-dependent homodyne detection is proposed to minimise the error in obtaining marginal distributions of different mechanical quadratures, from which we reconstruct the Wigner function of the quantum state in phase space. More specifically, for the same optomechanical device discussed above, the tomography error—quantifying the difference between the reconstructed Wigner function and the actual one—is given by the following covariance matrix:

$$\mathbf{V}_v = \frac{\hbar\zeta_F}{\sqrt{2}\,\eta}\begin{bmatrix} 2^{\frac{1}{4}}\sqrt{\alpha^2/(\zeta_F\hbar m)} & -1 \\ -1 & 2^{\frac{3}{4}}\sqrt{\zeta_F\hbar m/\alpha^2} \end{bmatrix}. \tag{42}$$

Notice that it is almost identical to the conditional covariance matrix $\mathbf{V}_s$ shown in Eq. (39), apart from that the off-diagonal terms have the opposite sign. The state steering can therefore be viewed as the time-reversal counterpart for state tomography, as the off-diagonal term flips sign when the oscillator momentum $\hat{p} \to -\hat{p}$ under $t \to -t$, and the condition for achieving a sub-Heisenberg error for state tomography— $\sqrt{\det \mathbf{V}_v} < \hbar/2$, is also identical to that for steerability.
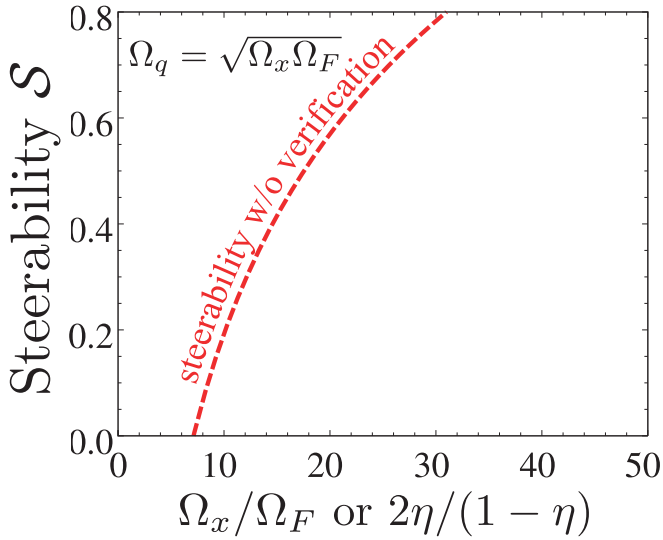
FIG. 6. Steerability $\mathscr{S}_v$ as a function of ratio Ω_x/Ω_F while keeping $\Omega_q = \sqrt{\Omega_x\Omega_F}$. Only the ratio between these frequencies determines the steerability, and the absolute values can vary depending on the chosen device.

Such a connection can be understood from the fact that for steering, one tries to prepare states with minimal uncertainty in certain quadratures $\hat{X}_\phi(0)$ with data from $(-\infty, 0]$—a *filtering* process, while for tomography, one tries to minimise the error in estimating quadratures $\hat{X}_\phi(0)$ with data from $(0, \infty)$—a *retrodiction* process. Due to linearity, both the minimal uncertainty and the tomography error for a given quadrature $\hat{X}_\phi$ all takes the quadratic form—$\boldsymbol{v}_\phi \mathbf{V}_{s,v} \boldsymbol{v}_\phi^{\mathrm{T}}$ and

$$\mathbf{V}_s = \mathbf{A} - \mathbf{C}^{\mathrm{T}}\mathbf{B}^{-1}\mathbf{C} \xrightarrow{\ t \to -t\ } \mathbf{V}_v. \qquad (43)$$

These two covariance matrixes $\mathbf{V}_{s,v}$ describe the remaining uncertainty in oscillator position $\hat{x}(0)$ and momentum $\hat{p}(0)$ conditional on both the amplitude $\hat{y}_1$ and phase quadrature $\hat{y}_2$ of optical field, for $t < 0$ and $t > 0$, respectively. Note that the above relation shown in Eq. (43) is exact only when the noise during the state preparation and the one during tomography are uncorrelated, as the correlation between them will break down the time-reversal symmetry, which happens if the cavity bandwidth is small and has noneligible memory time.

Verifiable steering and the experimental requirements. — Not only are the steering and tomography intimately related to each other, but also the tomography is necessary in order to verify the steering in the experiment. For Gaussian states, the tomography error simply adds on top of the covariance matrix for every conditional state. We therefore define the following figure of merit for verifiable quantum-state steering:

$$\mathscr{S}_v = -\ln\left[2\sqrt{\det[\mathbf{V}_s + \mathbf{V}_v]}/\hbar\right] = -\ln(2\zeta_F/\eta). \qquad (44)$$

We therefore require $\zeta_F < \eta/2$ for verifing quantum-state steering. It can be seen from comparing Fig. 2 and Fig. 6 that thermal noise from thermal fluctuation, and sensing noise from optical loss and quantum inefficiency, need to be at least

below the SQL in order to prepare and verify quantum-state steering. Noteworthy is the fact that steerability does not depend on the absolute value of the noise spectrum; one can therefore have the flexibility to choose the appropriate frequency range to carry out the experiment, depending on the specific setup.

The specific conditions for experimental demonstration of steering that we formulated here are scalable to any experimental setup. As Fig. 6 clearly demonstrates, the experimentalist should have a system where quantum noise dominates both thermal and sensing noise in a substantial frequency range. The ratio of $\Omega_x/\Omega_F \gtrsim 10$ should be provided to see steering in the experiment. Another important condition relates to measurement strength that has to be of the order of $\Omega_q = \sqrt{\Omega_x\Omega_F}$. In terms of quantum noise it means that radiation pressure noise should dominate over thermal fluctuations.

VI. CONCLUSION

We see that quantum entanglement exists universally in system with a mechanical oscillator coupled to the continuum of outgoing optical fields. The entanglement measure — logarithmic negativity displays an elegant scaling which depends on the ratio between characteristic interaction and thermal-noise frequency. Such scaling should also apply in electromechanical systems whose dynamics are similar to what we have considered. We also considered the possibility to use entanglement between light and mechanical motion for testing such a fundamental concept of quantum mechanic as steering. A close relation between steering and quantum state tomography procedure proposed in [32] is revealed. Our analysis once again confirms a well-known condition that experimental demonstration of macroscopic quantum effects in optomechanical systems, including EPR-type entanglement, requires the measurement apparatus to be quantum noise limited in some frequency band of interest. Furthermore, the measurement has to be strong enough to effectively extract information about the mechanical motion at a rate higher than that of a thermal decoherence which stipulates radiation pressure noise to dominate over the thermal and sensing noise in this frequency band. which is reflected in the relation between the characteristic frequencies we introduced: $\Omega_F < \Omega_q < \Omega_x$.

Appendix A: Wiener-Hopf method

In this appendix, we show how to derive $\mathbf{C}^{\mathrm{T}}\mathbf{B}^{-1}\mathbf{C}$ in Eq. (35), which is equivalent to solving an integral equation shown in Eq. (19), with the Wiener-Hopf method. We first show the general formalism and then specialise to the large-bandwidth and strong-measurement limit that we have considered.

1. General formalism

Here we first discuss the general formalism. In the continuous-time limit, $\mathbf{C}$ is a 2×2 matrix with elements given by $C_{ij}(t)$ and, similarly, the elements of $\mathbf{B}$ are $B_{ij}(t-t')$ ($i, j = 1, 2$) and they only depend on time difference due to stationarity). We define $\mathbf{K} = \mathbf{B}^{-1}\mathbf{C}$ or equivalently, $\mathbf{B}\mathbf{K} = \mathbf{C}$, and $\mathbf{K}$ is a 2×2 matrix with the elements satisfying the following integral equations:

$$\sum_{k=1}^{2} \int_{-\infty}^{0} dt' B_{ik}(t-t') K_{kj}(t') = C_{ij}(t), \qquad (A1)$$

and therefore, inverting $\mathbf{B}$ is equivalent to solving the above integral equation. Note that the upper limit of the integration is 0, instead of $+\infty$ in which case it can be solved simply by using Fourier transform. This arises naturally in the classical filtering problem with only past data that is available. The procedure for using Wiener-Hopf method to solve this set of integral equations goes as follows.

Firstly, we extend the definition of $K_{ij}(t)$ and $C_{ij}(t)$ to $t > 0$ but requiring $K_{ij}(t) = C_{ij}(t) = 0$ if $t > 0$, namely

$$K_{ij}(t) \rightarrow K_{ij}(t)\Theta(t), \quad C_{ij}(t) \rightarrow C_{ij}(t)\Theta(t), \qquad (A2)$$

This allows to extend the upper limit of the integral to be $+\infty$ without changing the result.

Secondly, we apply the Fourier transform

$$\tilde{f}(\omega) \equiv F[f(t)] = \int_{-\infty}^{+\infty} dt\, e^{i\omega t} f(t), \qquad (A3)$$

of the above equation and obtain

$$\left[\sum_{k=1}^{2} \tilde{B}_{ik}(\omega)\tilde{K}_{kj}(\omega) - \tilde{C}_{ij}(\omega) \right]_{-} = 0, \qquad (A4)$$

where $[f(\omega)]_{-}$ means the part of $\tilde{f}(\omega)$ that is analytical (no poles) in the upper-half complex plane by using the following decomposition:

$$\tilde{f}(\omega) \equiv [\tilde{f}(\omega)]_{+} + [\tilde{f}(\omega)]_{-}, \qquad (A5)$$

and $[f(\omega)]_{+}$ is the part that is analytical in the lower-half complex plane. From the definition of Fourier transform in Eq. (A3), the inverse Fourier transform of $[\tilde{f}(\omega)]_{-}$ vanishes for $t > 0$ from the residue theorem, namely

$$F^{-1}\left[[\tilde{f}(\omega)]_{-} \right] = f(t)\Theta(t) = 0, \quad \forall t > 0. \qquad (A6)$$

Let us focus on the equations associated with the first column of $\tilde{C}$, i.e., $j = 1$ (the situation for $j = 2$ will be similar), and we rewrite Eq. (A4) explicitly in terms of their components:

$$\left[\tilde{B}_{11}(\omega)\tilde{K}_{11}(\omega) + \tilde{B}_{12}(\omega)\tilde{K}_{21}(\omega) - \tilde{C}_{11}(\omega) \right]_{-} = 0, \quad (A7)$$

$$\left[\tilde{B}_{21}(\omega)\tilde{K}_{11}(\omega) + \tilde{B}_{22}(\omega)\tilde{K}_{21}(\omega) - \tilde{C}_{21}(\omega) \right]_{-} = 0. \quad (A8)$$

Thirdly, if $B_{11}(t) = B_{11}(-t)$, we can factorise $\tilde{B}_{11}(\omega)$ as

$$\tilde{B}_{11}(\omega) = \tilde{\varphi}_{+}(\omega)\tilde{\varphi}_{-}(\omega) \qquad (A9)$$

which is the Fourier counterpart of the Cholesky decomposition in time domain. We now can express $\tilde{K}_{11}(\omega)$ in terms of $\tilde{K}_{21}(\omega)$ in Eq. (A7). We use the fact that

$$[\tilde{f}(\omega)]_{-} = 0 \implies [\tilde{f}(\omega)\tilde{g}_{+}(\omega)]_{-} = 0, \forall \tilde{g} \qquad (A10)$$

Multiplying Eq. (A7) by $\varphi_{+}^{-1}(\omega)$, we get

$$\tilde{K}_{11} = \frac{1}{\tilde{\varphi}_{-}} \left[\frac{\tilde{C}_{11}}{\tilde{\varphi}_{+}} - \frac{\tilde{B}_{12}\tilde{K}_{21}}{\tilde{\varphi}_{+}} \right]_{-}. \qquad (A11)$$

Plugging it into Eq. (A8), we obtain

$$\left\{ \left[\tilde{B}_{22} - \frac{\tilde{B}_{21}\tilde{B}_{12}}{\tilde{B}_{11}} \right] \tilde{K}_{21} + \frac{\tilde{B}_{21}}{\tilde{\varphi}_{-}} \left[\frac{\tilde{C}_{11}}{\tilde{\varphi}_{+}} \right]_{-} \right.$$
$$\left. + \frac{\tilde{B}_{21}}{\tilde{\varphi}_{-}} \left[\frac{\tilde{B}_{12}\tilde{K}_{21}}{\varphi_{+}} \right]_{+} - \tilde{C}_{21} \right\}_{-} = 0 \qquad (A12)$$

where we have used the fact that:

$$\frac{\tilde{B}_{12}\tilde{K}_{21}}{\tilde{\varphi}_{+}} = \left[\frac{\tilde{B}_{12}\tilde{K}_{21}}{\tilde{\varphi}_{+}} \right]_{+} + \left[\frac{\tilde{B}_{12}\tilde{K}_{21}}{\tilde{\varphi}_{+}} \right]_{-}. \qquad (A13)$$

Again, if $\tilde{B}_{22} - \tilde{B}_{21}\tilde{B}_{12}/\tilde{B}_{11}$ is an even function of time—due to stationarity and time-reversal symmetry. We can make a similar factorization to the one shown in Eq. (A9):

$$\tilde{B}_{22}(\omega) - \frac{\tilde{B}_{21}(\omega)\tilde{B}_{12}(\omega)}{\tilde{B}_{11}(\omega)} = \tilde{\psi}_{+}(\omega)\tilde{\psi}_{-}(\omega). \qquad (A14)$$

The same as the approach for deriving Eq. (A11) by using the fact shown in Eq. (A10), we obtain

$$\tilde{K}_{21} = \frac{1}{\tilde{\psi}_{-}} \left[\frac{1}{\tilde{\psi}_{+}} \left(\tilde{C}_{21} - \frac{\tilde{B}_{21}}{\tilde{\varphi}_{-}} \left[\frac{\tilde{C}_{11}}{\tilde{\varphi}_{+}} \right]_{-} - \frac{\tilde{B}_{21}}{\tilde{\varphi}_{-}} \left[\frac{\tilde{B}_{12}\tilde{K}_{21}}{\tilde{\varphi}_{+}} \right]_{+} \right) \right]_{-}. \qquad (A15)$$

Note that in the above equation, $\tilde{K}_{21}$ appears in both sides of the equation, which might seems to be difficult to solve. Actually, since $\tilde{K}_{21}$ is analytical in the upper half complex plane, $[\tilde{B}_{12}\tilde{K}_{21}/\tilde{\varphi}_{+}]_{+}$ only depends on the value of $\tilde{K}_{21}$ at the poles of $\tilde{B}_{12}/\tilde{\varphi}_{+}$ in the upper-half complex plane. One only need to solve a set of simple algebra equations by evaluating the above equation on these poles.

2. Large-bandwidth and strong-measurement limit

In this section, we consider the case of the large-bandwidth and strong-measurement limit, and, for the oscillator, we have

$$\hat{x}(t) = \int_{-\infty}^{t} dt'\, G_x(t-t')[-\alpha \hat{a}_1(t') + \hat{F}_{\rm th}(t')], \qquad (A16)$$

$$\hat{p}(t) = m \int_{-\infty}^{t} dt'\, \dot{G}_x(t-t')[-\alpha \hat{a}_1(t') + \hat{F}_{\rm th}(t')], \qquad (A17)$$

and, for the output optical field, we have

$$\hat{y}_1(t) = \sqrt{\eta}\, \hat{a}_1(t) + \sqrt{1-\eta}\, \hat{n}_1(t), \qquad (A18)$$

$$\hat{y}_2(t) = \sqrt{\eta}\, [\hat{a}_2(t) + (\alpha/\hbar)\hat{x}(t)] + \sqrt{1-\eta}\, \hat{n}_2(t). \qquad (A19)$$

Here

$$G_x(t) = \frac{1}{m\omega_m} e^{-\kappa_m t/2} \sin \omega_m t \qquad (A20)$$

is the Green's function of the mechanical oscillator, and in the strong-measurement limit—the frequency at which we carry out the measurement is much higher than that of the mechanical frequency, the oscillator can be treated as a free mass and $G_x(t)|_{\rm free\ mass} = t/m$.

By using the fact that

$$\langle \hat{a}_j(t)\hat{a}_k(t')\rangle_{\rm sym} = \langle \hat{n}_j(t)\hat{n}_k(t')\rangle_{\rm sym} = \frac{1}{2}\delta_{jk}\delta(t-t') \quad (A21)$$

for $j,k = 1,2$, and

$$\langle \hat{F}_{\rm th}(t)\hat{F}_{\rm th}(t')\rangle_{\rm sym} = 2m\kappa_m k_B T \delta(t-t'), \qquad (A22)$$

we obtains the elements for covariance matrix $\mathbf{B}$ of $(\hat{y}_1, \hat{y}_2)$ in the frequency domain (spectral density):

$$\tilde{B}_{11}(\omega) = 1, \qquad (A23)$$

$$\tilde{B}_{12}(\omega) = -\eta \frac{\alpha^2}{\hbar} \tilde{G}_x^*(\omega), \qquad (A24)$$

$$\tilde{B}_{21}(\omega) = -\eta \frac{\alpha^2}{\hbar} \tilde{G}_x(\omega), \qquad (A25)$$

$$\tilde{B}_{22}(\omega) = 1 + \eta \frac{\alpha^2}{\hbar^2} \tilde{S}_{xx}(\omega), \qquad (A26)$$

and the correlation between $(\hat{y}_1, \hat{y}_2)$ and $(\hat{x}(0), \hat{p}(0))$:

$$\tilde{C}_{11}(\omega) = -\sqrt{\eta}\, \alpha \tilde{G}_x^*(\omega), \qquad (A27)$$

$$\tilde{C}_{12}(\omega) = -im\Omega\sqrt{\eta}\, \alpha \tilde{G}_x^*(\omega), \qquad (A28)$$

$$\tilde{C}_{21}(\omega) = \sqrt{\eta}\, \frac{\alpha}{\hbar} \tilde{S}_{xx}(\omega), \qquad (A29)$$

$$\tilde{C}_{22}(\omega) = im\Omega\sqrt{\eta}\, \frac{\alpha}{\hbar} \tilde{S}_{xx}(\omega), \qquad (A30)$$

where

$$\tilde{S}_{xx}(\omega) \equiv |\tilde{G}_x(\omega)|^2 (\alpha^2 + 4m\kappa_m k_B T), \qquad (A31)$$

and the Fourier transform for the mechanical Green's function is given by [strong-measurement limit is taken by setting $\kappa_m, \omega_m \to 0$]:

$$\tilde{G}_x(\omega) = \frac{-1}{m(\omega^2 - \omega_m^2 + i\kappa_m\omega)}. \qquad (A32)$$

In this case, we can easily carry out the factorization. For $\tilde{\varphi}_{\pm}(\omega)$ [cf. Eq. (A9)], we have

$$\tilde{\varphi}_+(\omega) = \tilde{\varphi}_-(\omega) = 1, \qquad (A33)$$

For $\tilde{\psi}_{\pm}(\omega)$ [cf. Eq. (A14)], we have

$$\tilde{\psi}_+(\omega)\tilde{\psi}_-(\omega) = 1 + \eta \frac{\alpha^2}{\hbar^2} |\tilde{G}_x^2(\omega)|^2 \left[(1-\eta)\alpha^2 + 4m\kappa_m k_B T \right]$$

$$= \frac{\omega^4 + (\kappa_m^2 - 2\omega_m^2)\omega^2 + \omega_m^4 + 2(\alpha^2/\hbar m)^2 \zeta_F^2}{\omega^4 + (\kappa_m^2 - 2\omega_m^2)\omega^2 + \omega_m^4}. \qquad (A34)$$

This leads to

$$\tilde{\psi}_+(\omega) = \tilde{\psi}_-^*(\omega) = \frac{(\omega - \omega_1)(\omega - \omega_2)}{(\omega - \omega_1')(\omega - \omega_2')}, \qquad (A35)$$

where ω_j and ω_j' $(j = 1,2)$ are the roots of the numerator and denominator of Eq. (A34) in the upper-half complex plane, respectively. Given the expression for $\tilde{\varphi}_{\pm}$ and $\tilde{\psi}_{\pm}$, we can solve $\tilde{K}_{ij}$ by using Eqs (A11), and Eq. (A15). This in turn allows us to obtain $\mathbf{V}_s = \mathbf{A} - \mathbf{C}^{\rm T}\mathbf{K}$ and in the time domain, it reads:

$$(\mathbf{V}_s)_{ij} = \mathbf{A}_{ij} - \sum_k \int_{-\infty}^{0} dt'\, C_{ki}(t') K_{kj}(t'), \qquad (A36)$$

from which we obtain Eq. (39).

[1] M. Aspelmeyer, P. Meystre, and K. Schwab, Physics Today **65**, 29 (2012), URL http://link.aip.org/link/?PTO/65/29/1.

[2] J. Chan, T. P. M. Alegre, A. H. Safavi-Naeini, J. T. Hill, A. Krause, S. Groblacher, M. Aspelmeyer, and O. Painter, Nature **478**, 89 (2011), ISSN 0028-0836, URL http://dx.doi.org/10.1038/nature10461.

[3] A. D. O'Connell, M. Hofheinz, M. Ansmann, R. C. Bialczak, M. Lenander, E. Lucero, M. Neeley, D. Sank, H. Wang, M. Wei-des, et al., Nature **464**, 697 (2010), ISSN 0028-0836, URL http://dx.doi.org/10.1038/nature08967.

[4] T. Purdy, R. Peterson, and R. C.A., arXiv:1209.6334 (2012), URL http://arxiv.org/abs/1209.6334.

[5] A. Einstein, B. Podolsky, and N. Rosen, Phys. Rev. **47**, 777 (1935).

[6] S. Mancini, V. Giovannetti, D. Vitali, and P. Tombesi, Phys. Rev. Lett. **88**, 120401 (2002), URL http://link.aps.org/doi/10.1103/PhysRevLett.88.120401.

[7] M. Pinard, A. Dantan, D. Vitali, O. Arcizet, T. Briant, and A. Heidmann, EPL (Europhysics Letters) **72**, 747 (2005), URL `http://stacks.iop.org/0295-5075/72/i=5/a=747`.

[8] D. Vitali, S. Gigan, A. Ferreira, H. R. Böhm, P. Tombesi, A. Guerreiro, V. Vedral, A. Zeilinger, and M. Aspelmeyer, Phys. Rev. Lett. **98**, 030405 (2007), URL `http://link.aps.org/doi/10.1103/PhysRevLett.98.030405`.

[9] M. Paternostro, D. Vitali, S. Gigan, M. S. Kim, C. Brukner, J. Eisert, and M. Aspelmeyer, Phys. Rev. Lett. **99**, 250401 (2007), URL `http://link.aps.org/doi/10.1103/PhysRevLett.99.250401`.

[10] H. Müller-Ebhardt, H. Rehbein, R. Schnabel, K. Danzmann, and Y. Chen, Phys. Rev. Lett. **100**, 013601 (2008), URL `http://link.aps.org/doi/10.1103/PhysRevLett.100.013601`.

[11] M. J. Hartmann and M. B. Plenio, Phys. Rev. Lett. **101**, 200503 (2008), URL `http://link.aps.org/doi/10.1103/PhysRevLett.101.200503`.

[12] H. Miao, S. Danilishin, H. Müller-Ebhardt, and Y. Chen, New Journal of Physics **12**, 083032 (2010), URL `http://stacks.iop.org/1367-2630/12/i=8/a=083032`.

[13] H. Miao, S. Danilishin, and Y. Chen, Phys. Rev. A **81**, 052307 (2010), arXiv:0908.1053.

[14] H. M. Wiseman, S. J. Jones, and A. C. Doherty, Phys. Rev. Lett. **98**, 140402 (2007), URL `http://link.aps.org/doi/10.1103/PhysRevLett.98.140402`.

[15] S. J. Jones, H. M. Wiseman, and A. C. Doherty, Phys. Rev. A **76**, 052116 (2007), URL `http://link.aps.org/doi/10.1103/PhysRevA.76.052116`.

[16] D. J. Saunders, S. J. Jones, H. M. Wiseman, and G. J. Pryde, Nat Phys **6**, 845 (2010), URL `http://dx.doi.org/10.1038/nphys1766`.

[17] H. M. Wiseman and J. M. Gambetta, Phys. Rev. Lett. **108**, 220402 (2012), URL `http://link.aps.org/doi/10.1103/PhysRevLett.108.220402`.

[18] F. Marquardt, J. P. Chen, A. A. Clerk, and S. M. Girvin, Phys. Rev. Lett. **99**, 093902 (2007), URL `http://link.aps.org/doi/10.1103/PhysRevLett.99.093902`.

[19] I. Wilson-Rae, N. Nooshi, W. Zwerger, and T. J. Kippenberg, Phys. Rev. Lett. **99**, 093901 (2007), URL `http://link.aps.org/doi/10.1103/PhysRevLett.99.093901`.

[20] C. Genes, D. Vitali, P. Tombesi, S. Gigan, and M. Aspelmeyer, Phys. Rev. A **77**, 033804 (2008), URL `http://link.aps.org/doi/10.1103/PhysRevA.77.033804`.

[21] D. Walls and G. Milburn, *Quantum optics* (Springer, 2008).

[22] H. Müller-Ebhardt, H. Rehbein, C. Li, Y. Mino, K. Somiya, R. Schnabel, K. Danzmann, and Y. Chen, Physical Review A (Atomic, Molecular, and Optical Physics) **80**, 043802 (pages 18) (2009), URL `http://link.aps.org/abstract/PRA/v80/e043802`.

[23] A. Barchielli, International Journal of Theoretical Physics **32**, 2221 (1993), ISSN 0020-7748, URL `http://dx.doi.org/10.1007/BF00672994`.

[24] G. J. Milburn, Quantum and Semiclassical Optics: Journal of the European Optical Society Part B **8**, 269 (1996), URL `http://stacks.iop.org/1355-5111/8/i=1/a=019`.

[25] A. Hopkins, K. Jacobs, S. Habib, and K. Schwab, Phys. Rev. B **68**, 235328 (2003), URL `http://link.aps.org/doi/10.1103/PhysRevB.68.235328`.

[26] A. C. Doherty, S. M. Tan, A. S. Parkins, and D. F. Walls, Phys. Rev. A **60**, 2380 (1999), URL `http://link.aps.org/doi/10.1103/PhysRevA.60.2380`.

[27] A. C. Doherty and K. Jacobs, Phys. Rev. A **60**, 2700 (1999), URL `http://link.aps.org/doi/10.1103/PhysRevA.60.2700`.

[28] V. Braginsky and F. Khalili, *Quantum Measurement* (Cambridge University Press, Cambridge, 1992).

[29] R. F. Werner and M. M. Wolf, Phys. Rev. Lett. **86**, 3658 (2001), URL `http://link.aps.org/doi/10.1103/PhysRevLett.86.3658`.

[30] G. Adesso and F. Illuminati, Journal of Physics A: Mathematical and Theoretical **40**, 7821 (2007), URL `http://stacks.iop.org/1751-8121/40/i=28/a=S01`.

[31] G. Vidal and R. F. Werner, Phys. Rev. A **65**, 032314 (2002), URL `http://link.aps.org/doi/10.1103/PhysRevA.65.032314`.

[32] H. Miao, S. Danilishin, H. Müller-Ebhardt, H. Rehbein, K. Somiya, and Y. Chen, Phys. Rev. A **81**, 012114 (2010).